Electronic Supplementary Material (ESI) for Dalton Transactions.

A Cu(II) metallocycle for the reversible self-assembly of coordination-driven polyrotaxane-like architectures

Giada Truccolo,[†] Zeno Tessari,[†] Jacopo Tessarolo,[‡] Silvio Quici,[§] Lidia Armelao,*[†,‡] Marzio Rancan*[,‡]

Electronic Supplementary Information

[†] *Department of Chemical Sciences, University of Padova, via Marzolo 1, 35131 Padova, Italy*

[‡] *Institute of Condensed Matter Chemistry and Technologies for Energy (ICMATE), National Research Council (CNR), c/o Department of Chemical Sciences, University of Padova, via Marzolo 1, 35131 Padova, Italy*

[§] *Institute of Molecular Science and Technologies (ISTM), National Research Council (CNR), Via C. Golgi 19, 20133 Milano*

e-mail: marzio.rancan@unipd.it; marzio.rancan@cnr.it
lidia.armelao@unipd.it

Index

Tables

Figures

1. Synthesis of ligand L

1.1 Synthesis of 1-{4-[(4-acetylphenyl)methyl]phenyl}ethan-1-one (preL)

Diphenylmethane (1.68 g, 10 mmol) has been dissolved in 30 mL of dry CS_2, in a 100 mL 3 necks round bottom flask, under nitrogen atmosphere. $AlCl_3$ (3.47 g, 26 mmol) has been added to the solution, under vigorous stirring. The reaction mixture has been cooled to 0 °C, then a solution of acetyl chloride (1.85 mL, 26 mmol) in 5 mL of CS_2 has been added. The mixture has been stirred at room temperature for 30 minutes, then it has been reacted at reflux temperature for 3 hours. After that, the solvent has been removed under reduced pressure and 100 g of ice, together with 25 mL of HCl 12 M, have been added to the remaining solid. The mixture has been extracted with CH_2Cl_2 (150 mL) and the organic phase has been collected. The organic phase has been washed with a 5% $NaHCO_3$ aqueous solution (100 mL) and then with a saturated NaCl aqueous solution (80 mL). The organic phase has been dried over $MgSO_4$ and the solvent has been removed under reduced pressure resulting in 3.3 g of pale yellow solid. The product has been purified by SiO_2 column chromatography (*n*-hexane/ethyl acetate 6:4) to give 1.7 g (yield 67.5%) of white solid.

^{1}H-NMR (400MHz, $CDCl_3$, T = 25°C): δ [ppm] = 7.89 (4H, AA' part of an AA'BB' m, $H_{2,2'}$), 7.27 (4H, BB' part of an AA'BB' m, $H_{3,3'}$), 4.09 (2H, s, H_4), 2.58 (6H, s, H_1).

Elemental analysis for **preL** ($C_{17}H_{16}O_2$), experimental (calculated): C 80.45% (80.93%), H 6.54% (6.39%).

Figure S1. ^{1}H-NMR (400MHz, $CDCl_3$, 25°C) spectrum of **preL**.

1.2 Synthesis of 1-(4-{[4-(3-oxo-3-phenylpropanoyl)phenyl]methyl}phenyl)-3-phenylpropane-1,3-dione (L)

preL (1.51 g, 6 mmol) has been dissolved in 30 mL of dry DMF, in a 100 mL 3 necks round bottom flask, under nitrogen atmosphere. To this solution, ethyl benzoate (3.5 mL, 24 mmol) and potassium *tert*-butoxide (2.02 g, 18 mmol) have been added, maintaining the solution at room temperature and under vigorous stirring. The mixture have been stirred at room temperature for 16 hours (overnight). After this time, water (100 mL) and an HCl 10% aqueous solution, have been added to the solution. The mixture has been extracted with ethyl acetate (200 mL) and the organic phase has been collected. The organic phase has been washed with water (2 x 100 mL), dried over $MgSO_4$ and the solvent has been removed under reduced pressure resulting in 2.40 g of a white solid. The product has been purified by recrystallization from 25 mL of CH_3CN to give 1.7 g of pure product with quantitative yield. Compound purity has been confirmed by NMR, ESI-MS, ATR, SCXRD and elemental analysis.

^{1}H-NMR (400MHz, $CDCl_3$, T = 25°C): δ [ppm] = 16.88 (2H, s, H_5), 7.98 (4H, BB' part of an AA'BB' m, $H_{3,3'}$), 7.94 (4H, AA' part of an AA'BB' m, $H_{6,6'}$), 7.55 (2H, m, H_1), 7.49 (4H, AA' part of an AA'BB' m, $H_{2,2'}$), 7.32 (4H, BB' part of an AA'BB' m, $H_{7,7'}$), 6.84 (2H, s, H_4), 4.13 (2H, s, H_8).

^{13}C-NMR (400MHz, $CDCl_3$, T = 25°C): δ [ppm] =185.58, 185.53 (s, C_5, C_7), 145.13 (s, C_{11}), 135.52 (s, C_4), 133.85 (s, C_8), 132.47 (s, C_1), 129.35 (s, C_{10}), 128.71 (s, C_2), 127.61 (s, C_9), 127.16 (s, C_3), 93.02 (s, C_6), 41.86 (s, C_{12}).

ESI-MS (negative mode, acetonitrile): $[(\mathbf{L})\text{-H}]^-$ = 459.30 m/z (459.16 m/z calculated)

ATR (cm^{-1}): 3058 w br, 2921 w, 2900 w,1589 m br, 1520 m, 1481 m br, 1299 m br, 1227 m, 1184 m, 1120 w, 1059 w, 1026 w, 1018 w, 1000 w, 924 w, 872 w, 838 w br, 802 w, 777 w, 751 s, 698 m, 683 s, 655 m, 638 m, 616 w, 593 m br.

Elemental analysis for **L** ($C_{31}H_{24}O_4$), experimental (calculated): C 80.74% (80.85%), H 5.32% (5.25%).

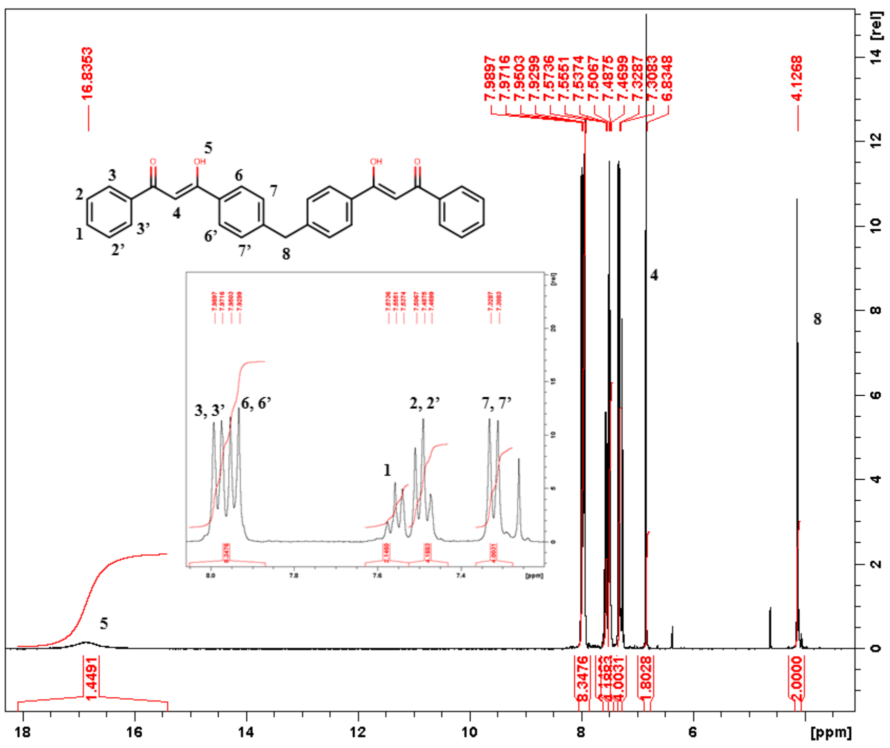

Figure S2. ^{1}H-NMR (400MHz, $CDCl_3$, 25°C) spectrum of **L**.

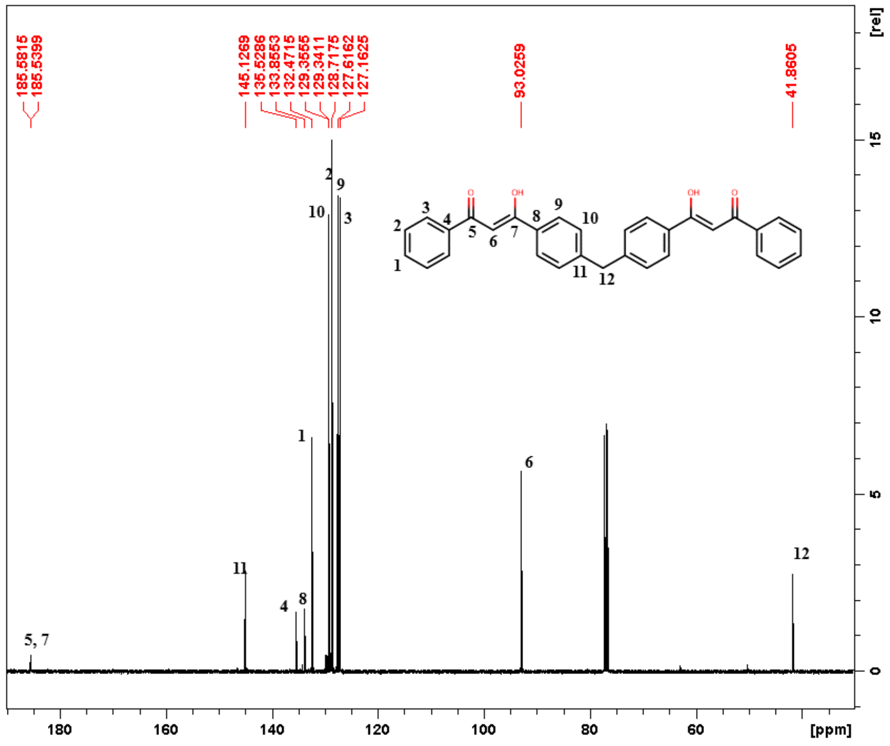

Figure S3. ^{13}C-NMR (400MHz, $CDCl_3$, 25°C) spectrum of **L**.

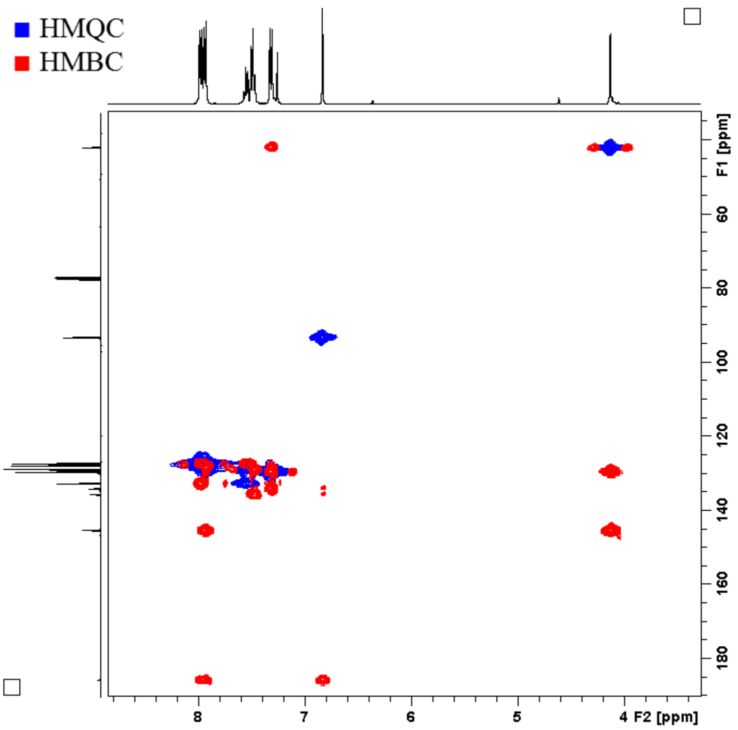

Figure S4. HMQC (400MHz, $CDCl_3$, 25°C, blue) spectrum and HMBC (400MHz, $CDCl_3$, 25°C, red) spectrum of **L**.

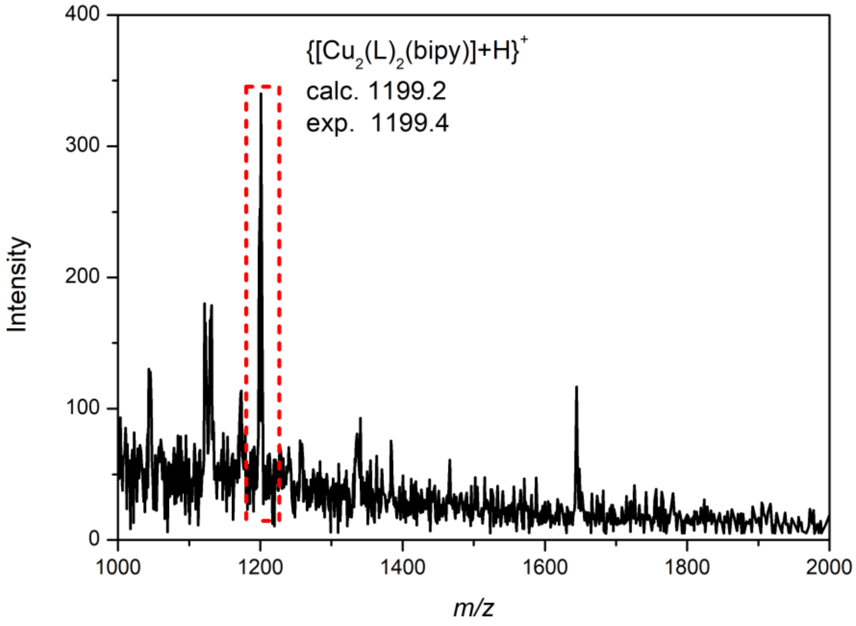

Figure S5. ESI-MS (positive mode, THF) of a diluted **1** solution (THF, 10^{-5} M) plus a bipy stoichiometric amount $\{[Cu_2(L)_2](bipy) + H\}^+$ = 1199.4 m/z (1199.2 m/z calculated).

2. Powder X-ray diffraction (SCXRD)

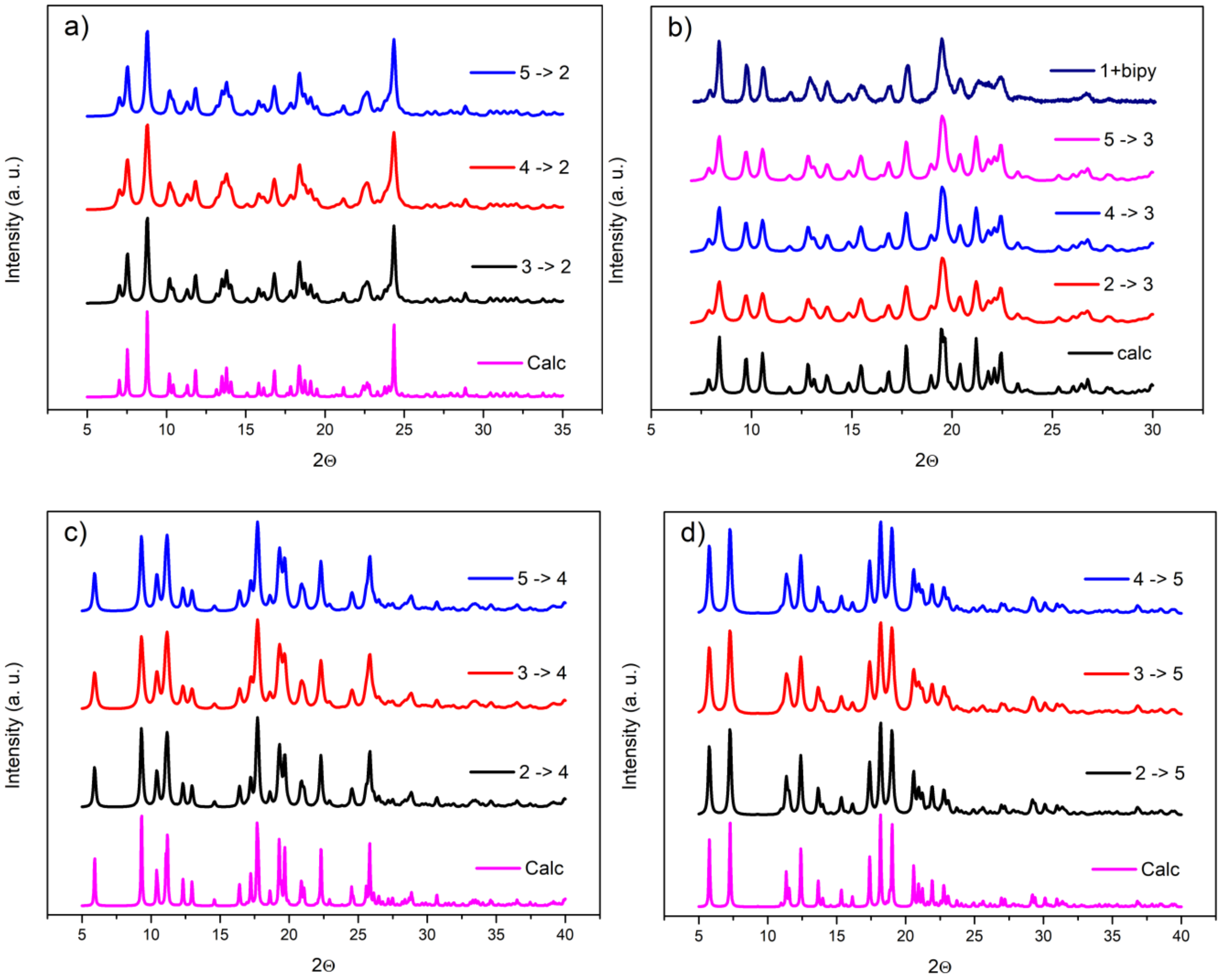

Figure S6. PXRD patterns of the obtained products from interconversion experiments. a) *n* → 2 (*n* = 3, 4, 5); b) *n* → 3 (*n* = 2, 4, 5) and “1+bipy” is the product of reaction at section 2.3 (method B); c) *n* → 4 (*n* = 2, 3, 5); c) *n* → 5 (*n* = 2, 3, 4).

3. Single crystal X-ray diffraction (SCXRD)

Single crystals of compounds have been fastened on the top of a Lindemann glass capillary, a nylon loop or mounted using Paratone-N oil and centered on the head of a four circle kappa goniometer Oxford Diffraction Gemini E diffractometer, equipped with a 2K × 2K EOS CCD area detector and sealed-tube Enhance (Mo) and (Cu) X-ray sources. Data have been collected by means of the ω-scans technique using graphite-monochromated radiation. Detector distance has been set at 45 mm. The diffraction intensities have been corrected for Lorentz/polarization effects as well as with respect to absorption. Empirical multi-scan absorption corrections using equivalent reflections have been performed with the scaling algorithm SCALE3 ABSPACK. Data reduction, finalization and cell refinement were carried out through the CrysAlisPro software. Accurate unit cell parameters were obtained by least squares refinement of the angular settings of strongest reflections, chosen from the whole experiment. In all the cases, structures were solved by means of intrinsic phasing method using SHELXT[2] and refined by full-matrix least squares methods based on F_o^2 with SHELXL-97[2] in the framework of OLEX2 software.[3] In the last cycles of refinement, ordered nonhydrogen atoms were refined anisotropically whereas disordered partial occupancy non-hydrogen atoms were refined isotropically. Hydrogen atoms connected to carbon atoms were included in idealized positions, and a riding model was used for their refinement. A summary of the crystallographic data and of the refinement parameters for each compound is provided in the following sections and in Table S11.

3.1 Ligand L refinement details

Single crystals of **L** were obtained from a dichloromethane/toluene solution containing 3 mg of triphenylphophine oxide (TPPO). Mo Kα (λ = 0.71073 Å) radiation was used for data collection. Structural solution and refinement were carried out as described above.

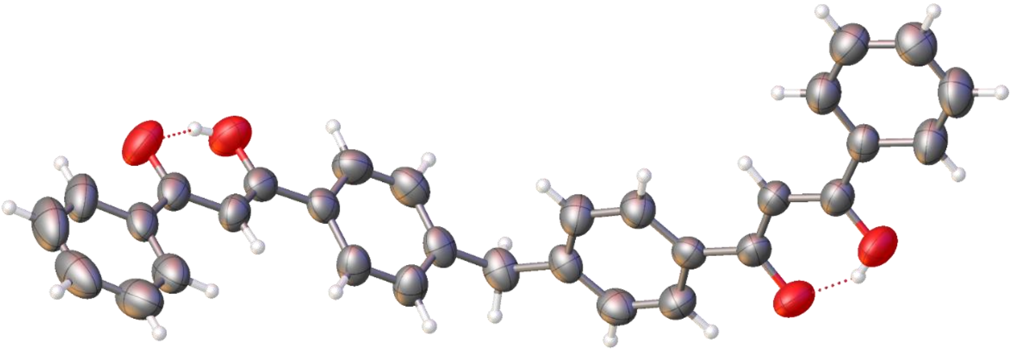

Figure S7. Asymmetric unit for ligand **L**, thermal ellipsoid drawn at the 50% level. Colour code: O red, C grey, H white.

3.2 $\{[Cu_2(L)_2]\cdot 2(CHCl_3)\}$ ($1\cdot 2CHCl_3$) refinement details

Single crystals of **1** have been obtained by reactant diffusion technique. Mo Kα (λ = 0.71073 Å) radiation was used for data collection. Crystals showed rapid degradation if exposed to air due to loss of crystallization solvent. Low temperature measurements have been performed (150 ± 1 K). Structural solution and refinement were carried out as described above.

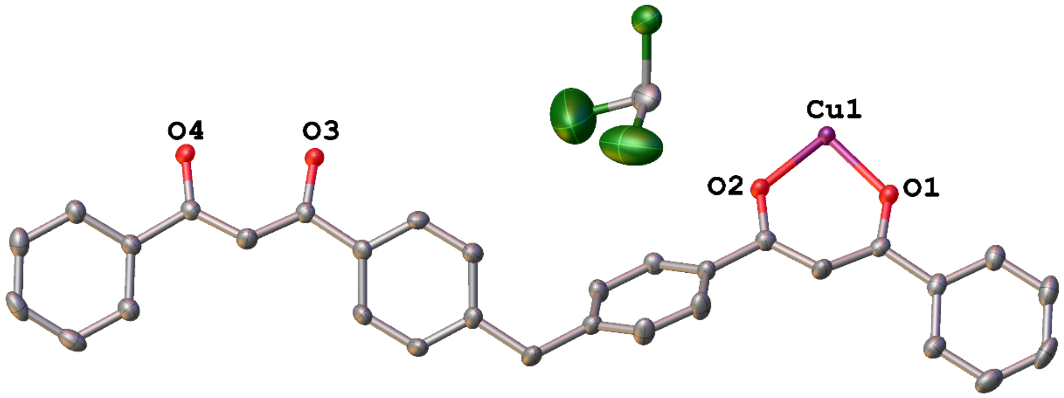

Figure S8. Asymmetric unit of **1** with thermal ellipsoids drawn at the 50% probability level. Colour code: Cu purple, O red, C grey, Cl dark green, H omitted for clarity.

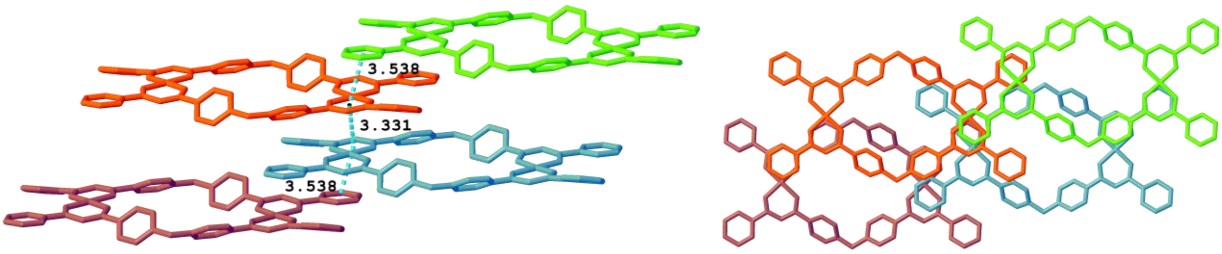

Figure S9. Stacking interactions between the terminal phenyl rings of ligands and the rings formed by the metallo-β-diketonate moiety ("CuO_2C_3"). Two different interactions are present: the first involves two "CuO_2C_3" rings (3.3 Å) and the second is between a "CuO_2C_3" ring and a phenyl ring (3.5 Å).

Table S1. Selected bond distances in **1.**

Atom 1	**Atom 2**	**Distance (Å)**	**Atom 1**	**Atom 2**	**Distance (Å)**
Cu1	O1	1.911(3)	Cu1	O4[1]	1.910(3)
Cu1	O3[1]	1.911(3)	Cu1	O2	1.909(3)

[1] 1-X,1-Y,1-Z

Table S2. Selected angles in **1**.

Atom 1	**Atom 2**	**Atom 3**	**Angle (˚)**	**Atom 1**	**Atom 2**	**Atom 3**	**Angle (˚)**
O1	Cu1	O3[1]	179.19(14)	O2	Cu1	O1	93.67(13)
O4[1]	Cu1	O1	86.75(13)	O2	Cu1	O3[1]	85.76(13)
O4[1]	Cu1	O3[1]	93.86(13)	O2	Cu1	O4[1]	177.01(15)

[1] 1-X,1-Y,1-Z

3.3 {[$Cu_2(L)_2$]($DMA)_2$} (2) refinement details

Single crystals of **2** were obtained from DMA after slow diffusion of diethyl ether vapours. Mo Kα (λ = 0.71073 Å) radiation was used for data collection. Structural solution and refinement were carried out as described above. DFIX restrains have been applied to selected bonds (O5-C32 = 1.2 ± 0.005 Å, N1-C32 = 1.3 ± 0.005 Å, C33-C32 = 1.5 ± 0.005 Å) to better model the DMA molecule. RIGU restrain has been applied to DMA atoms.

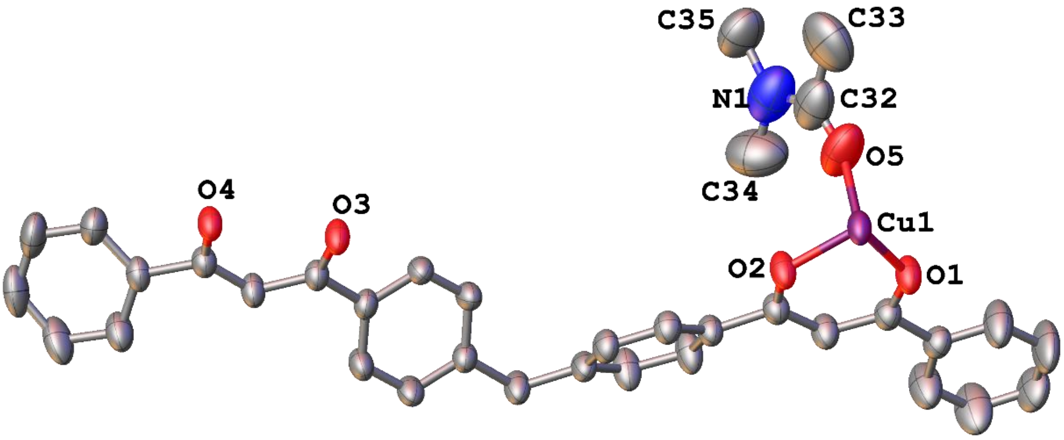

Figure S10. Asymmetric unit of **2** with thermal ellipsoids drawn at the 50% probability level. Colour code: Cu purple, O red, C grey, N blue, H omitted for clarity.

Table S3. Selected bond distances in **2**.

Atom 1	Atom 2	Distance (Å)	Atom 1	Atom 2	Distance (Å)
Cu1	O4[1]	1.9312(18)	Cu1	O1	1.925(2)
Cu1	O2	1.9270(19)	Cu1	O5	2.268(3)
Cu1	O3[1]	1.9210(19)			

[1] 1-X,1-Y,1-Z

Table S4. Selected angles in **2**.

Atom 1	Atom 2	Atom 3	Angle (˚)	Atom 1	Atom 2	Atom 3	Angle (˚)
O4[1]	Cu1	O5	98.48(12)	O3[1]	Cu1	O1	177.00(10)
O2	Cu1	O4[1]	169.28(10)	O3[1]	Cu1	O5	91.07(12)
O2	Cu1	O5	92.23(13)	O1	Cu1	O4[1]	87.30(8)
O3[1]	Cu1	O4[1]	92.85(8)	O1	Cu1	O2	92.73(8)
O3[1]	Cu1	O2	86.56(8)	O1	Cu1	O5	91.87(12)

[1] 1-X,1-Y,1-Z

3.4 {[Cu_2(L)$_2$](bipy)}$_n$ (3) refinement details

Single crystals of **3** have been obtained by reactant diffusion technique. Mo Kα (λ = 0.71073 Å) radiation was used for data collection. Structural solution and refinement were carried out as described above. A terminal phenyl ring of the ligand was disordered over two sites, the occupancies of which were constrained to sum to 1.0. The terminal phenyl ring was modelled using SADI (± 0.01), FLAT, SIMU and RIGU commands.

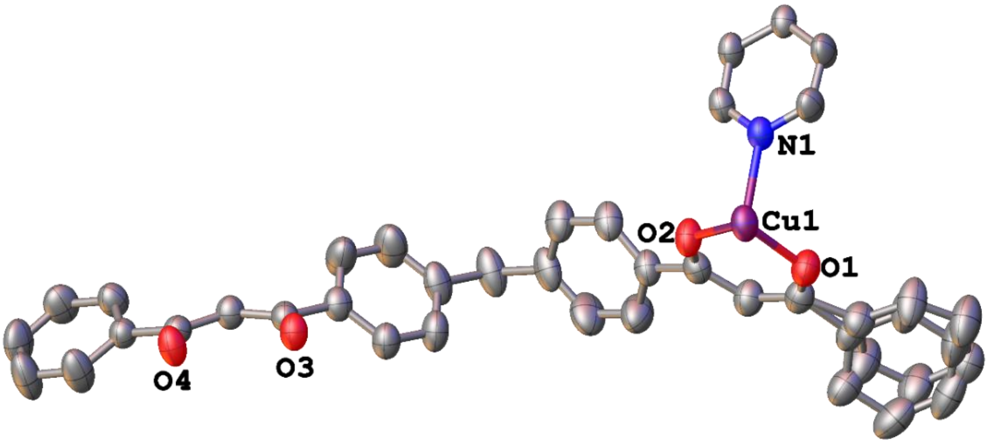

Figure S11. Asymmetric unit of **3** with thermal ellipsoids drawn at the 50% probability level. Colour code: Cu purple, O red, C grey, N blue, H omitted for clarity.

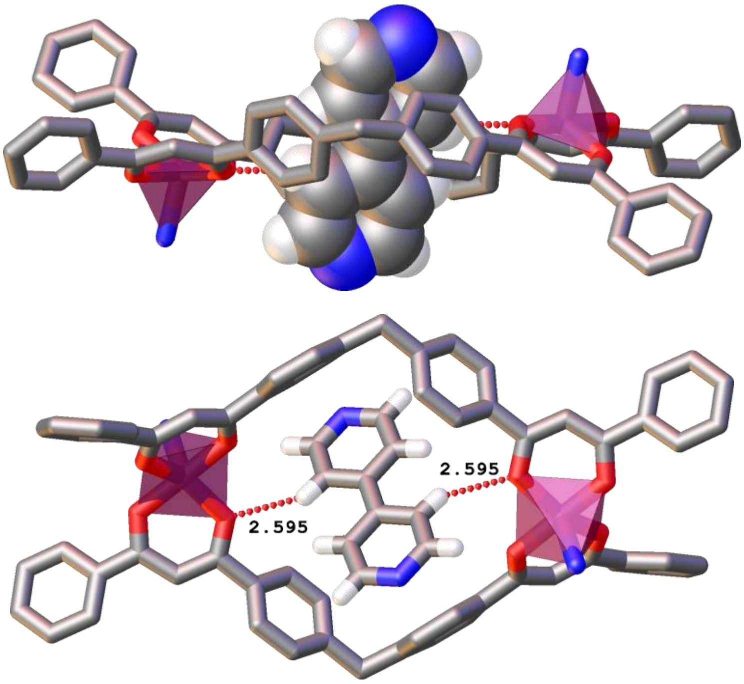

Figure S12. Bipy hosted in the metallocycle pocket lateral and top views. Colour code: Cu purple, O red, C grey, N blue, metallocycle H atoms omitted for clarity.

Table S5. Selected bond distances in **3**.

Atom 1	Atom 2	Distance (Å)	Atom 1	Atom 2	Distance (Å)
Cu1	$O3^1$	1.979(2)	Cu1	O1	1.959(2)
Cu1	O2	1.935(2)	Cu1	N1	2.212(3)
Cu1	$O4^1$	1.934(2)			

^{1}1-X,-Y,1-Z

Table S6. Selected angles in **3**.

Atom 1	Atom 2	Atom 3	Angle (˚)	Atom 1	Atom 2	Atom 3	Angle (˚)
$O3^1$	Cu1	N1	112.27(10)	$O4^1$	Cu1	O2	177.82(10)
O2	Cu1	$O3^1$	90.78(10)	$O4^1$	Cu1	O1	85.83(11)
O2	Cu1	O1	92.07(10)	$O4^1$	Cu1	N1	90.25(11)
O2	Cu1	N1	90.74(11)	O1	Cu1	$O3^1$	145.81(11)
$O4^1$	Cu1	$O3^1$	90.65(10)	O1	Cu1	N1	101.75(11)

^{1}1-X,-Y,1-Z

3.5 {[$Cu_2(L)_2$]$(py)_2$} (4) refinement details

Single crystals of **4** were obtained from a 1:1 DMA/py after slow evaporation. Mo Kα (λ = 0.71073 Å) radiation was used for data collection. Structural solution and refinement were carried out as described above.

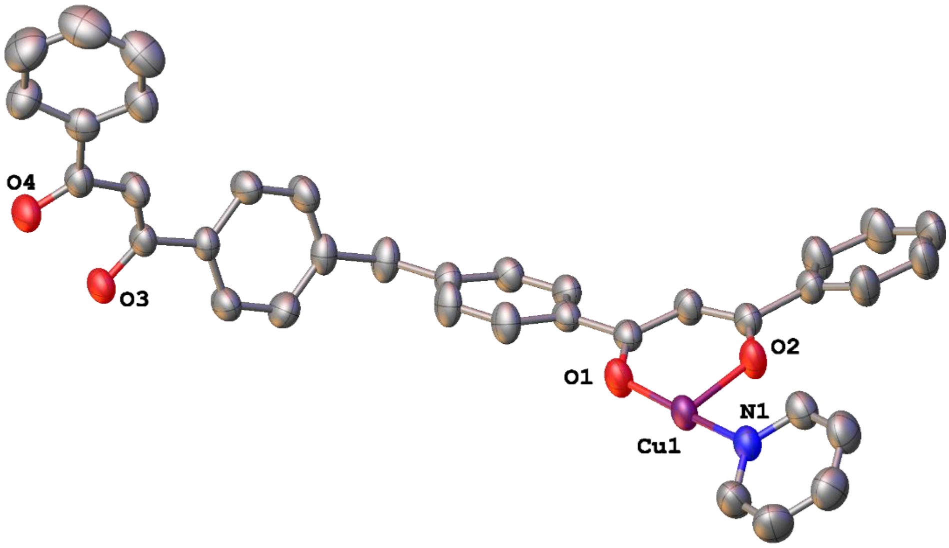

Figure S13. Asymmetric unit of **4** with thermal ellipsoids drawn at the 50% probability level. Colour code: Cu purple, O red, C grey, N blue, H omitted for clarity.

Table S7. Selected bond distances in **4**.

Atom 1	Atom 2	Distance (Å)	Atom 1	Atom 2	Distance (Å)
Cu1	$O3^1$	1.974(2)	Cu1	$O4^1$	2.173(2)
Cu1	O1	1.931(2)	Cu1	N1	2.027(3)
Cu1	O2	1.928(2)			

^{1}1-X,1-Y,1-Z

Table S8. Selected angles in **4**.

Atom 1	Atom 2	Atom 3	Angle (°)	Atom 1	Atom 2	Atom 3	Angle (°)
$O3^1$	Cu1	$O4^1$	89.38(9)	O2	Cu1	$O3^1$	161.49(11)
$O3^1$	Cu1	N1	89.76(10)	O2	Cu1	O1	91.76(10)
O1	Cu1	$O3^1$	85.89(9)	O2	Cu1	$O4^1$	109.09(10)
O1	Cu1	$O4^1$	92.96(10)	O2	Cu1	N1	90.80(10)
O1	Cu1	N1	173.40(11)	N1	Cu1	$O4^1$	91.96(11)

^{1}1-X,-Y,1-Z

3.6 {[$Cu_2(L)_2$](DMA)(phpy)} (5) refinement details

Single crystals of **5** were obtained from DMA after slow diffusion of diethyl ether vapours. The obtained crystals were very small despite several efforts to increase their dimensions. The analysed specimen was a blade-like crystals with 0.08 × 0.03 × 0.01 mm dimensions. This strongly affects the quality of the final structure (CHECKCIF: 1 Alert level B: Low Bond Precision on C-C Bonds 0.02438 Ang; several Alert level C). However the data quality is sufficient to properly determine chemical connectivity and crystal packing. Mo Kα (λ = 0.71073 Å) radiation was used for data collection. Structural solution and refinement were carried out as described above. Ligand terminal phenyl rings were disordered over two sites, the occupancies of which were constrained to sum to 1.0. These disordered rings were modelled using the following restrains: SADI (± 0.01), FLAT and RIGU. To selected rings atoms (C26B C26A C27A C27B and C28B C29B C28A C29A) EADP constrain was applied. The same constrain was used for the phenyl-pyridine carbon atoms. The Flack parameter was refined to 0.46(4). This value, close to 0.5, suggests that the crystal consists of a racemic mixture of the two enantiomers. Hence the structure was refined as a 2-component inversion twin.

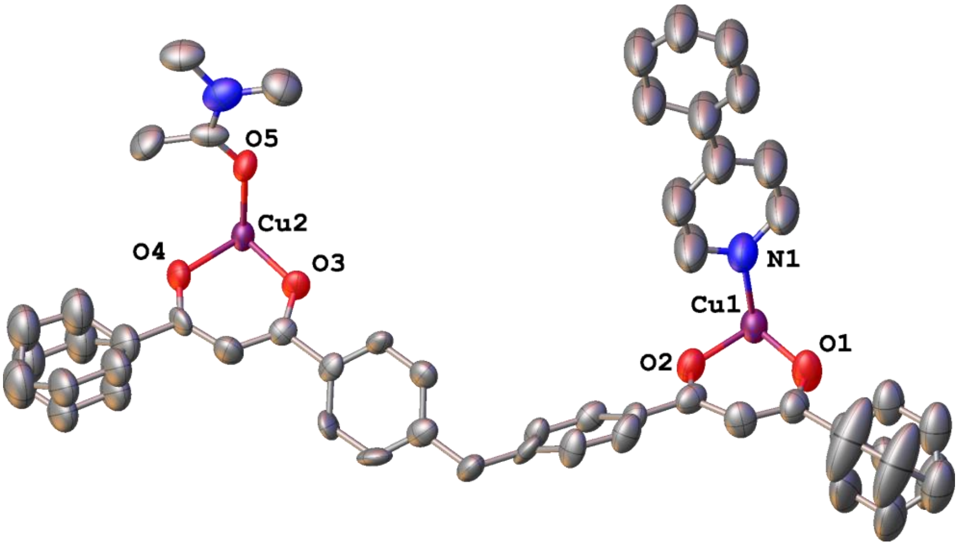

Figure S14. Asymmetric unit of **5** with thermal ellipsoids drawn at the 50% probability level. Colour code: Cu purple, O red, C grey, N blue, H omitted for clarity.

Table S9. Selected bond distances in **5**.

Atom 1	Atom 2	Distance (Å)	Atom 1	Atom 2	Distance (Å)
Cu1	O2	1.933(10)	Cu2	O3^{1}	1.961(8)
Cu1	O2^{1}	1.933(10)	Cu2	O3	1.961(8)
Cu1	N1	2.276(14)	Cu2	O4	1.956(8)
Cu1	O1^{1}	1.928(10)	Cu2	O4^{1}	1.956(8)
Cu1	O1	1.928(10)	Cu2	O5	2.199(13)

^{1}1-X,+Y,+Z

Table S10. Selected angles in **5**.

Atom 1	Atom 2	Atom 3	Angle (˚)	Atom 1	Atom 2	Atom 3	Angle (˚)
O2^{1}	Cu1	O2	86.4(6)	O3	Cu2	O3^{1}	86.2(5)
O2	Cu1	N1	92.2(5)	O3^{1}	Cu2	O5	97.8(3)
O2^{1}	Cu1	N1	92.2(5)	O3	Cu2	O5	97.8(3)
O1^{1}	Cu1	O2	167.1(5)	O4^{1}	Cu2	O3^{1}	91.7(3)
O1^{1}	Cu1	O2^{1}	92.1(4)	O4	Cu2	O3	91.7(3)
O1	Cu1	O2^{1}	167.1(5)	O4	Cu2	O3^{1}	164.8(4)
O1	Cu1	O2	92.1(4)	O4^{1}	Cu2	O3	164.8(4)
O1	Cu1	N1	100.6(5)	O4^{1}	Cu2	O4	86.4(6)
O1^{1}	Cu1	N1	100.6(5)	O4	Cu2	O5	97.4(4)
O1	Cu1	O1^{1}	86.5(6)	O4^{1}	Cu2	O5	97.4(4)

^{1}1-X,+Y,+Z

Table S11. Crystallographic details

Compound	**L**	**1**	**2**	**3**	**4**	**5**
CCDC	1844084	1844080	1844082	1844085	1844081	1844083
Formula	$C_{31}H_{24}O_4$	$C_{32}H_{23}Cl_3CuO_4$	$C_{35}H_{31}CuNO_5$	$C_{36}H_{26}CuNO_4$	$C_{36}H_{27}CuNO_4$	$C_{38.5}H_{29}CuNO_{4.5}$
$D_{calc.}$/ g cm^{-3}	1.297	1.551	1.355	1.413	1.425	1.340
m/mm^{-1}	0.085	1.125	0.775	0.817	0.822	0.731
Formula Weight	460.50	641.39	609.15	600.12	601.12	641.17
Colour	colourless	dark green	light green	light green	clear light green	clear intense green
Shape	plate	needle	needle	needle	plate	irregular
Size/mm^3	0.50×0.30×0.08	0.30×0.15×0.05	0.20×0.03×0.01	0.30×0.05×0.01	0.18×0.12×0.05	0.08×0.03×0.01
T/K	296.6(3)	150.00(10)	298.3(6)	298.8(4)	296.8(9)	298(1)
Crystal System	monoclinic	triclinic	triclinic	triclinic	triclinic	orthorhombic
Flack Parameter	-0.1(5)	---	---	---	---	0.46(4)
Hooft Parameter	-0.3(4)					0.463(12)
Space Group	P2$_1$	P-1	P-1	P-1	P-1	Cmc2$_1$
a/Å	11.7464(12)	9.9134(6)	10.0967(8)	9.7072(5)	9.5306(2)	24.2987(16)
b/Å	5.2568(3)	11.5595(7)	11.7663(6)	12.5827(7)	10.9270(2)	8.5438(5)
c/Å	19.2835(13)	13.3769(7)	12.5885(9)	13.7631(8)	15.9767(4)	30.614(3)
a/°	90	111.662(5)	88.775(5)	63.589(6)	70.823(2)	90
b/°	98.150(8)	96.458(5)	88.996(7)	70.337(5)	89.045(2)	90
g/°	90	100.561(5)	87.429(6)	76.509(5)	64.357(2)	90
V/Å^3	1178.70(16)	1373.03(15)	1493.47(18)	1410.82(16)	1401.25(6)	6355.6(8)
Z	2	2	2	2	2	8
Z'	1	1	1	1	1	1
Wavelength/Å	0.71073	0.71073	0.71073	0.71073	0.71073	0.71073
Radiation type	MoK$_{a}$	MoK$_{\alpha}$	MoK$_{\alpha}$	MoK$_{\alpha}$	MoK$_{\alpha}$	MoK$_{\alpha}$
Q_{min}/°	2.562	2.436	2.347	2.429	2.417	2.527
Q_{max}/°	26.366	26.372	26.373	26.372	26.371	24.712
Measured Refl.	17085	11096	11363	10586	11035	14602
Independent Refl.	4816	5574	5943	5765	5731	5085
Reflections Used	3557	4567	3876	4309	4541	3681
R_{int}	0.0236	0.0339	0.0620	0.0412	0.0405	0.0608
Parameters	318	361	382	434	379	409
Restraints	1	42	35	331	0	197
Largest Peak	0.110	1.100	1.063	0.624	0.889	0.514
Deepest Hole	-0.110	-1.841	-0.760	-0.323	-0.396	-0.404
GooF	1.045	1.086	1.080	1.063	1.051	1.127
wR_2 (all data)	0.0995	0.2332	0.2435	0.1366	0.1696	0.2215
wR_2	0.0868	0.2161	0.2066	0.1235	0.1533	0.2018
R_1 (all data)	0.0650	0.0887	0.1289	0.0915	0.0711	0.1354
R_1	0.0416	0.0732	0.0864	0.0657	0.0557	0.1001

4. FT-IR

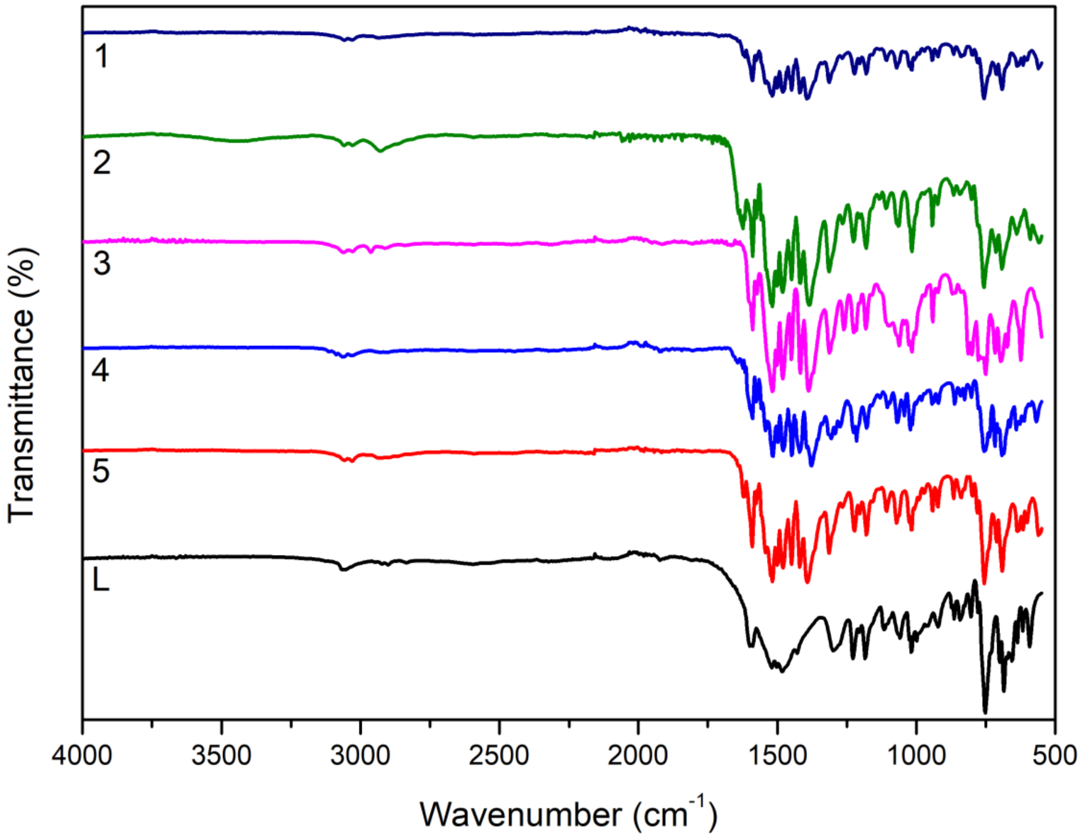

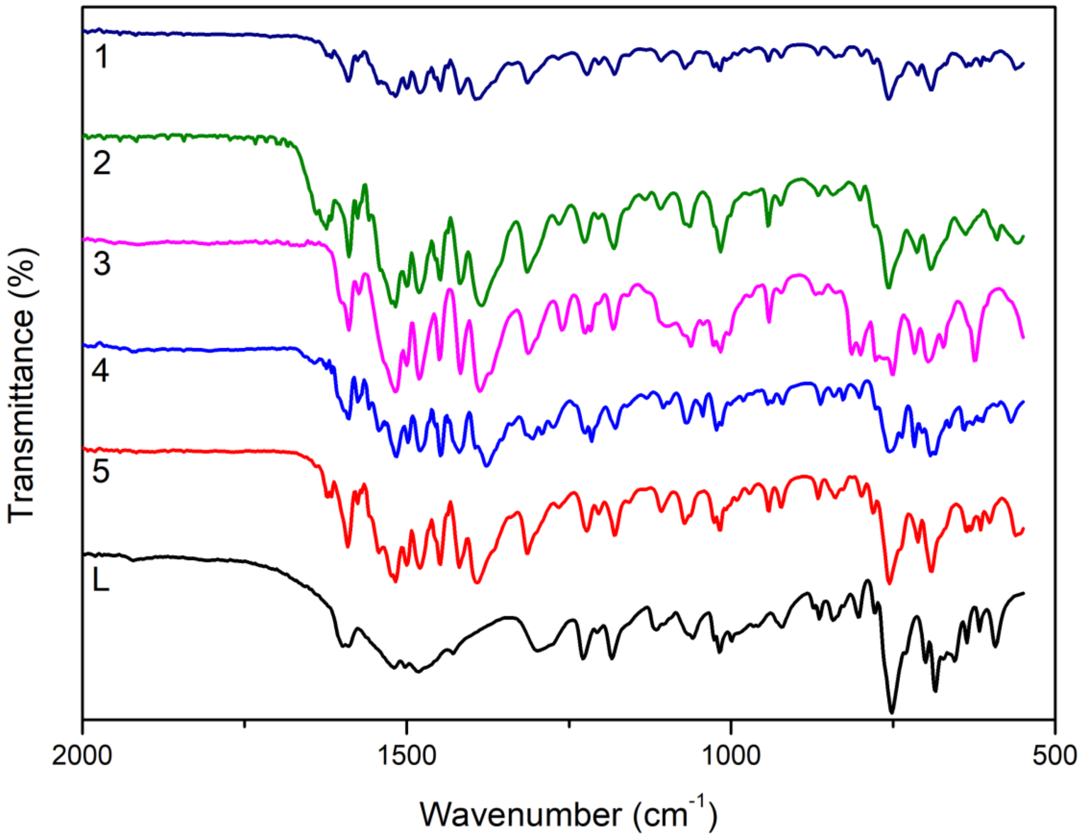

Figure S15. FT-IR spectra (upper 4000-500 cm^{-1}, bottom 2000-500 cm^{-1}) of the coordination compounds and the ligand L.

5. References

1. Dolomanov, O.V., Bourhis, L.J., Gildea, R.J, Howard, J.A.K. & Puschmann, H. (2009), J. Appl. Cryst. 42, 339-341.
2. Sheldrick, G.M. (2015). Acta Cryst. A71, 3-8.
3. Sheldrick, G.M. (2015). Acta Cryst. C71, 3-8.